Petrography and Petrogenesis of a Mid-Ocean Ridge Lava Suite

Matthew C. Smith and Michael R. Perfit
University of Florida Department of Geological Sciences

Over 60% of the Earth's magma flux, > 21 km^3/yr, takes place at mid-ocean ridges (MOR). These divergent plate boundaries are the loci of volcanism and plutonism that form the oceanic crust, which covers over 70% of Earth's surface. Mid-ocean ridge magmas typically undergo less modification and differentiation from their original primary melt composition than magmas erupted in continental settings or at oceanic islands. With a less complicated history, these MOR lavas provide a clearer window into mantle melting and magma chamber processes. Much insight into many different magmatic rock suites can be gained by understanding the magmatic processes involved in the formation of mid-ocean ridge lavas and determining their petrogenetic histories.

The major rock type recovered at MOR is basalt. In fact, because it is so common, basalt found at spreading ridges are called MORB, or mid-ocean ridge basalts. Other terms that have commonly been used to describe MORB include ocean ridge basalts (ORB), abyssal tholeiites, ocean ridge tholeiites and low-K olivine tholeiites, implying certain compositional characteristics.

In this investigation you will examine the petrography and geochemistry of 6 samples of mid-ocean ridge basalt and related differentiated lavas recovered from the Cleft segment of southern Juan de Fuca Ridge (JdFR), a medium spreading-rate MOR in the northeast Pacific Ocean (Figure 1). The goals of this investigation are to:

1. Investigate magmatism in a mid-ocean ridge environment
2. Examine petrography and mineralogy of tholeiitic igneous systems
3. Relate observed textures and mineral phases to relevant basalt phase diagrams and magma evolution
4. Correlate observed mineralogic changes with magma chemical evolution
5. Investigate how chemical variations may correlate with MOR/tectonic environment.

A brief introduction to the geology and tectonics of the Cleft Segment of the JdFR, and MORB petrography, in general, follows. More detailed descriptions can be found in Stakes et al. (2006) and Smith et al. (1994).

The Cleft Segment of the Juan de Fuca Ridge

The Cleft Segment of the southern Juan de Fuca Ridge (JdFR) is a highly symmetrical intermediate-rate spreading center (~6 cm/yr full rate) with a well-defined axial valley cut by the 30-90 m wide, 10-15 m deep, "cleft" that extends ~10 km along the center of the axial valley in the southern portion of the segment (Fig. 1, 2) [*Normark et al.*, 1986, 1987, Stakes et al., 2006]. The "cleft" is an axial collapse trough where fissure-fed eruptions are focused within the axial valley of the ridge.

Sm

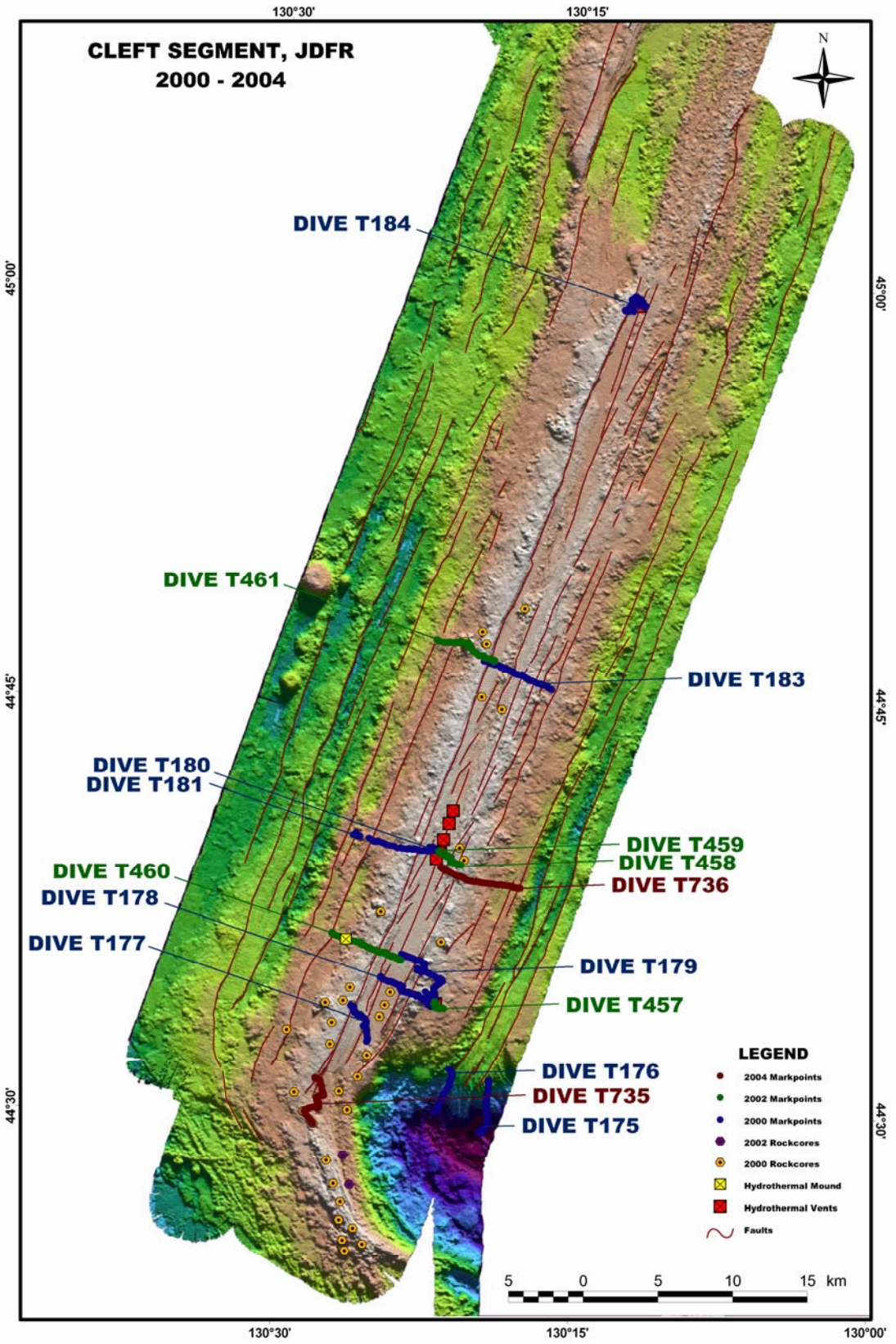

Figure 1: Bathymetric map of the Cleft Segment of the Juan de Fuca Ridge after Stakes et al., 2006 Figure 1. Locations of ROV dives made between 2000 and 2004 are shown along with sample locations and other relevant features (see legend)

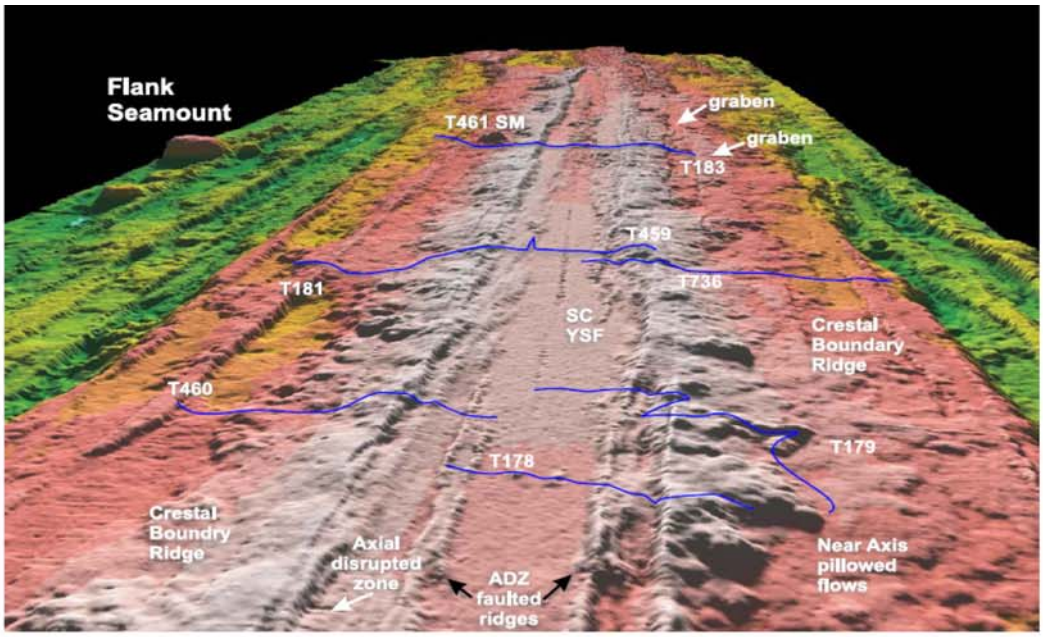

Figure 2: (above) 3-d perspective bathymetric map (looking north) of the southern Cleft Segment (below) close-up of ridge-axis bathymetry illistrating central cleft with interpretive drawing below southern cleft topography (after Stakes et al., 2006 Figure 2 (above) and Figure 3 (below)

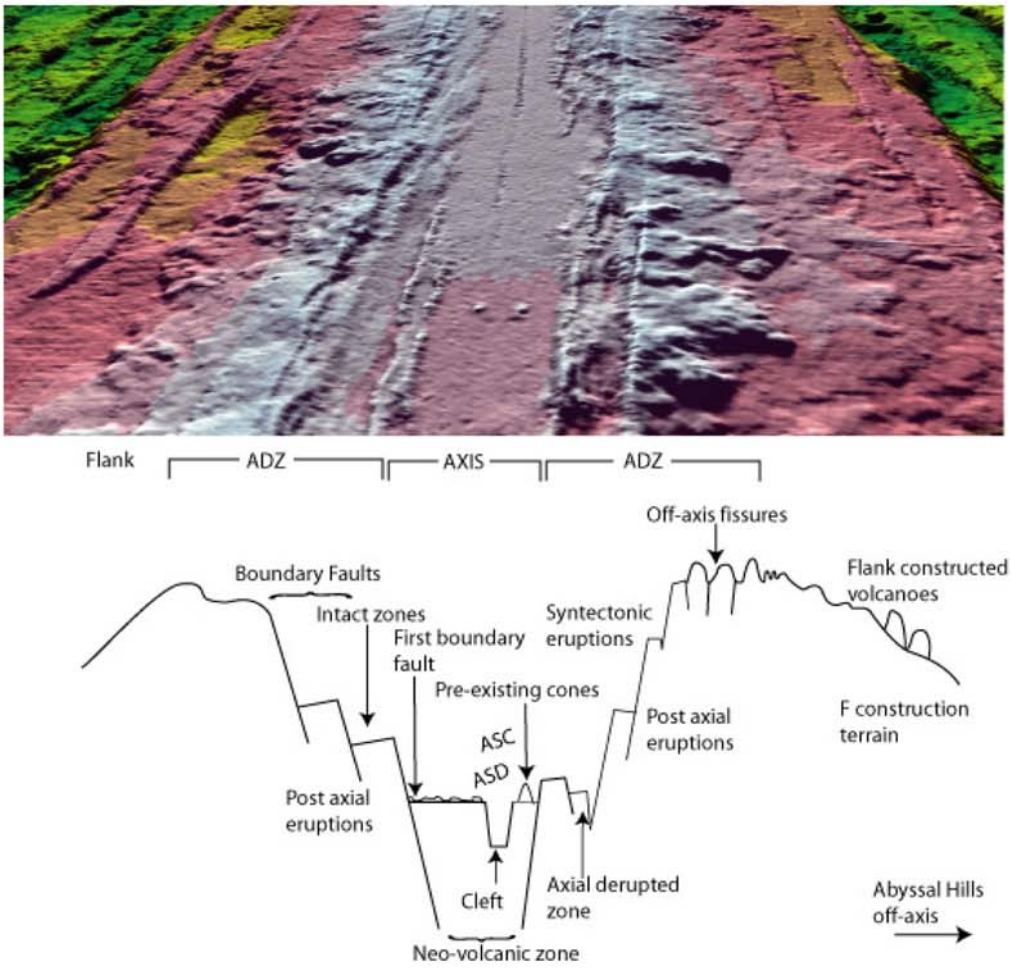

The central "cleft" is morphologically (and perhaps genetically) identical to the ***axial summit collapse trough*** (ASCT) described for the magmatically robust East Pacific Rise (EPR) [*Fornari et al., 1998*].

Similar to the fast-spreading, magmatically robust northern EPR, recent volcanism and active high-temperature hydrothermal sites are concentrated in a narrow <100m wide zone around the "cleft" [*Normark et al.*, 1983; 1986; 1987; *Embley et al.*, 1991; *Embley and Chadwick*, 1994; *Perfit and Chadwick*, 1998]. The cleft is known to have been volcanically active over the past several decades, and has recently erupted lobate, sheet and massive flows (Fig. 1) [*Normark et al.*, 1987, *Embley et. al.*, 1991, *Embley and Chadwick*, 1994]. North and south of the area with a central "cleft", the axial morphology changes to a more subdued axial valley dominated by thick, linear, pillow mounds; features similar to the axial volcanic ridges (AVR) common on slow spreading ridges [*Chadwick and Embley*, 1994; *Smith et al.*, 1999; *Head et al.*, 1996]. The volcanically and hydrothermally active axial valley is similar, although not identical to, the axial rift valleys or graben of slow spreading centers. The axial valley is bounded by 75-200 meter high "bow-form" ridges, postulated as vestiges of split, axial volcanoes (Fig. 1) [*Kappel and Ryan*, 1986]. These "split ridges" are suggested to delineate periods of robust axial volcanism followed by periods of tectonic extension. Thus, according to the split volcano hypothesis most of the magmatism at the Cleft Segment occurs at the axis, with cyclic oscillations between robust volcano building and waning periods of largely amagmatic faulting, extension and disruption [Smith et al., 1994].

The largely symmetrical and structurally simple southern Juan de Fuca Ridge was created as a result of a tectonically complex history of propagating rifts and changes in plate motion associated with the breakup and subduction of the Farallon plate beneath North America [*Wilson*, 1988; *Wilson et al.*, 1984]. Based on the youngest magnetic anomaly patterns, the southward propagation of the southernmost Juan de Fuca ceased approximately 1.4 Mybp with abrupt terminations at the Blanco Transform Zone (BTZ) [*Embley and Wilson*, 1992]. The BTZ has undergone several northward jumps at this intersection in concert with the conjugate processes of rift propagation and failure. *Embley and Wilson* [1992] suggest that the most recent readjustment was a northward jump at approximately 0.4 million years ago. The JdFR-BTZ ridge-transform intersection is characterized by an abrupt termination of the BTZ against a hummocky and inflated ridge crest that overshoots and hooks around the deep transform to the south (Fig. 1).

Figure 3 shows the locations for the MOR lavas you will examine as part of this investigation as well as the locations of recovered basalt samples reported in the PetDB geochemical database, an online geochemical database of rocks from the ocean floor [http://www.petdb.org]. MOR lavas for this study (except sample JdF90-DR12a-2) were all recovered in situ from the southern portion of the Cleft Segment using the submersible *Alvin* (operated by the National Deep Submergence Facility [NDSF] at Woods Hole Oceanographic Institution) or the remotely operated vehicle (ROV) *Tiburon (owned and operated by the Monterey Bay Aquarium Research Institute).* All of the lavas were recovered either within the Axial valley or off-axis from the nearby surrounding ridge flanks. As such, these samples are all relatively young, postdating any

of the ridge-axis readjustments described above. Sample DR12a-2 was recovered from the ridge axis of the southernmost portion of the Vance segment, the JdFR segment immediately north of the Cleft segment.

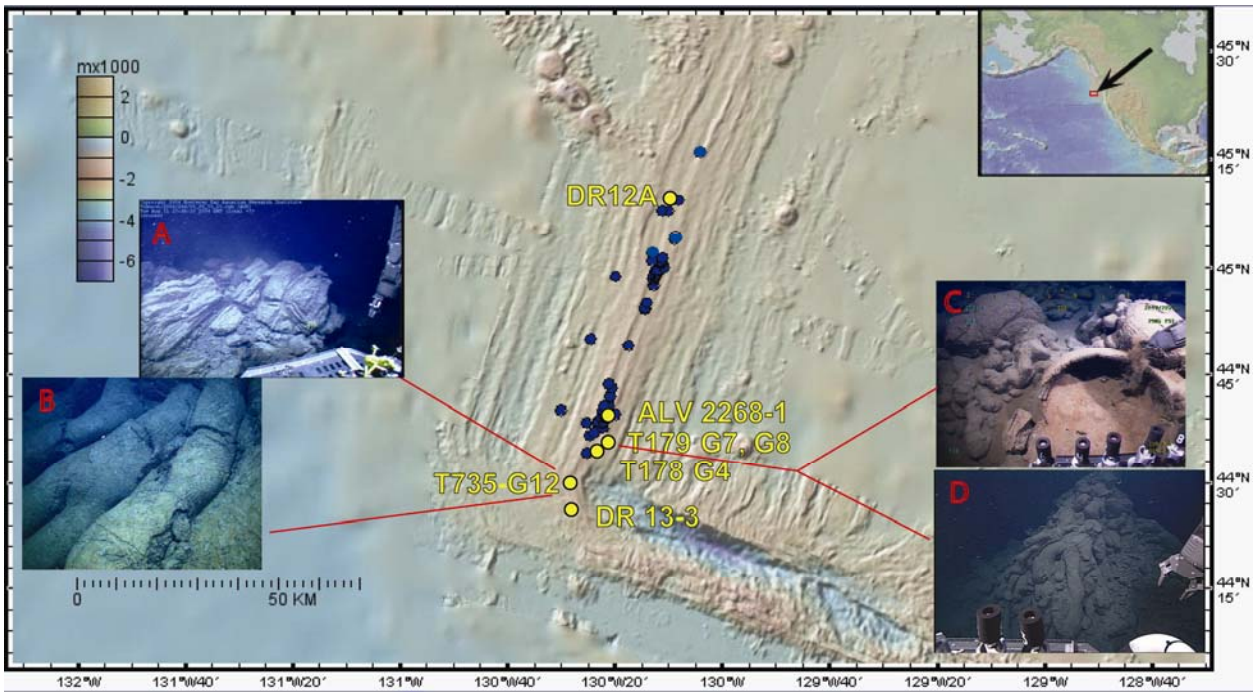

Figure 3: Sothern Juan De Fuca ridge showing locations of samples thin-sectioned for this investigation (yellow circles) and other MORB reported in the PetDB database [http://www.petdb.org]. Upper right inset shows location of map. Inset Photo A shows the dacite dome structure from which sample T735-12 was recovered. Photo B shows large andesitic to dacitic pillow tubes. Photo C shows a collapsed pillow and D shows a small hornito at the recovery sites of samples T179-G7 and T179-G8 respectively.

MORB Petrography: Mineralogy

Normative- Normative mineralogy is a theoretical mineralogy calculated on the basis of the major/minor element chemistry of the rock (these elements, occurring as oxides generally, each make up greater than ~0.1% of the total rock by weight). The CIPW normative calculation is one such technique. This technique recasts the rock chemistry into a set of idealized standard "normative minerals". The normative mineralogy or "norm" provides a ready means to compare and classify different rocks based on their chemistry, and can be particularly useful in the case where the rocks are very fine-grained or glassy. Note that normative mineralogy does not necessarily correlate to the modal mineralogy, which is the mineral makeup of the rock that is actually observed (typically expressed as the volume %). This is particularly true for glassy rocks, as crystallization was halted before completion, making classification based on observed mineralogy difficult. MORB (and other basalts) can be classified using the calculated CIPW norm and basalt tetrahedron (a basalt classification scheme based on normative mineralogy) [Morse, 1981]. The basalt tetrahedron (Figure 4) is a quaternary system that includes the minerals forsterite, diopside, nepheline, and quartz as the 4 end-member minerals. Enstatite and Albite are intermediate phases in this system. Basalts can be classified into several different groups using this scheme. These classifications primarily relate to the degree of silica (SiO_2) saturation in the magma (other classification schemes for basalts use the relative abundance of alkali elements (K, Na), trends of iron enrichment, or other parameters).

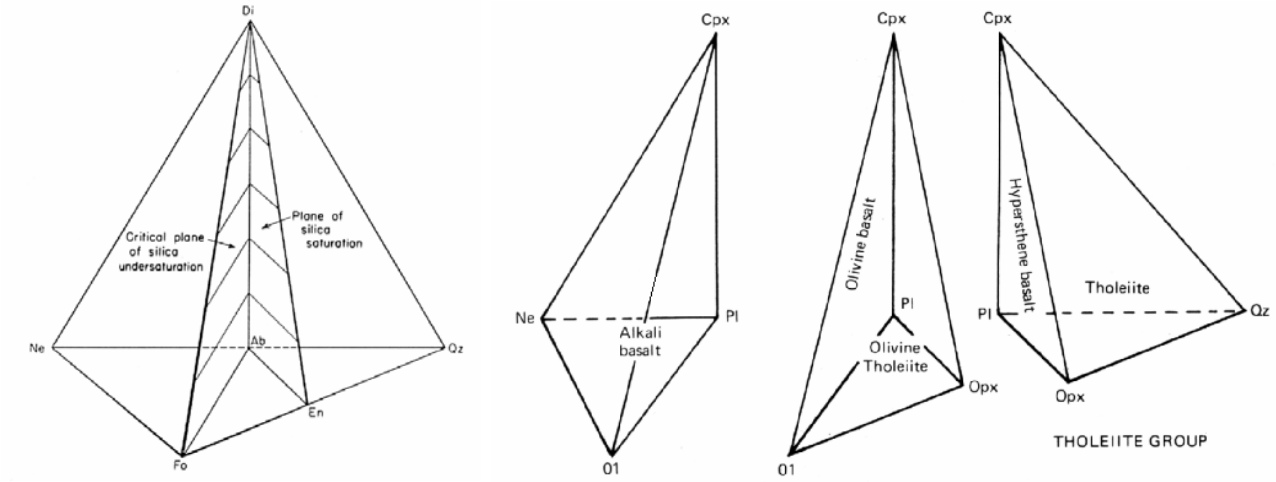

Figure 4: Basalt tetrahedron (Morse, 1981)

The basalt tetrahedron divides basalts into two major classes that can then be further subdivided. The two fundamental divisions are alkalic basalts and tholeiitic basalts. Alkalic basalts are critically undersaturated with respect to silica (nepheline occurs in the normative mineralogy), whereas subalkaline, tholeiitic basalts range from oversaturated (quartz in the norm) with respect to silica to undersaturated (olivine, but no Ne in the norm). Those without quartz in their norm are known as olivine tholeiites

or transitional basalts. The differences between alkalic and tholeiitic basalts are at least in part an artifact of the conditions of mantle melting that produced the primary magmas. Typically differentiates of these two basalt types stay within their respective fields on the basalt tetrahedron. (i.e. differentiates of alkali basalts continue to plot in the Ne-normative field and differentiates of tholeiites remain in the tholeiite field, though and ol. tholeiite can evolve into a quartz tholeiite.) These two magma lineages form two distinctive magma series, each sharing a unique petrogenesis.

Modal Mineralogy- The three principal phases typically found in MORB are plagioclase (plag), olivine (ol), and augitic clinopyroxene (cpx). Commonly, olivine and plagioclase occur as phenocryst phases. Clinopyroxene appears as a phenocryst in MORB that has evolved significantly from its primitive composition. More often, clinopyroxene occurs as a groundmass phase in association with plagioclase ± olivine ± oxides. In highly evolved MORB, orthopyroxene or pigeonite (sub-calcic clinopyroxene) can replace olivine as a significant mineral phase. Plagioclase compositions usually range from labradorite (An_{50}) to anorthite, except in the most chemically evolved lavas. Fe-Ti bearing oxides (titano-magnetite, for example) are common, but they typically crystallize late in the cooling of a lava (they are typically groundmass phases). However, in MORB magmas that have been highly enriched in FeO as a result of tholeiitic magma evolution, oxide crystallization can be stabilized earlier in the crystallization sequence and may form phenocrsts (e.g. Perfit and Fornari, 1983).

MORB Petrography: Textures

Textures and modal mineralogy can be related to cooling history and to the phase relationships detailed in simplified phase diagrams that relate to basaltic systems. Hence, mineralogic and textural relationships provide information on magma chemistry and conditions of crystallization. There is a connection! Sometimes, events such as the recharge of a magma chamber with a new batch of primitive magma or mixing of magmas with distinctly different compositions can be deduced by carefully observing the textures (and compositions) of mineral grains (primarily phenocryst phases.)

There are many textures that one can observe in MORB (and other rocks) that provide information about the cooling history of the lava [Natland, 1980; Bryan, 1983; Grove, 1990]. MORB are usually erupted at temperatures ~1200°C into water that is typically about 2° C leading to cooling so rapid (quenching) that crystals have little time to grow or nucleate at all. This rapid quenching leads to a variety of groundmass and microphenocryst textures that are characteristic of eruption in an aqueous environment. Typically MORB are glassy to fine-grained and rarely contain more than 10% phenocrysts. Lava morphology (related to eruption dynamics) plays a large role in the textural development of MORB, and rocks can range from holohyaline (exterior surfaces of flows or entire sheet flows if thin enough) to fine-grained holocrystalline (interiors of thicker flows, common in pillow lavas) and more rarely to porphyritic textures. Intergranular textures are very common, including intergrowths of mafic minerals (olivine, pyroxene) with plagioclase. Eruptive dynamics and the flow of lava can lead to sub-trachytic textures (*aligned crystals*) and elongate vesicles.

Vesicle size and shape has implications about the amount exsolved volatiles within the lava, which relates to lava chemistry, eruption environment and eruptive style. Generally, however, MORB tend to have a low vesicularity (<2%) compared to subaerially erupted lavas because MORB magmas have low volatile contents by comparison, and the pressure of the overlying water column inhibits bubble formation and vesiculation. If water depth (pressure) is held constant, vesicle size and abundance generally correlates with how evolved a lava is, because volatile (H_2O, CO_2) contents generally increase with increasing magma evolution. Rocks as evolved as andesites and dacites occur rarely in MOR settings, and as expected, have a greater volume of vesicles. Vesicle walls are often "decorated" with magmatic sulfides that crystallize within them, and with time, vesicles may become completely filled with secondary (not magmatic) minerals, in which case the vesicles are termed amygdules.

Holohyaline rocks and glassy crusts imply rapid cooling and are inherently unstable and devitrify with time. Commonly, quenched MORB will display several key textures that reveal this rapid cooling (as opposed to basalts erupted subaerially, that cool more slowly). These quench textures include radially grown plagioclase and pyroxene in fascicular (*bundle-like*) to variolitic (*spherical radial crystal growths*) intergrowths. In addition incomplete crystallization during rapid cooling also result in crystals with swallow-tail structures and hopper forms. Figure 5 shows pictures of some of these textures.

Phenocrysts typically comprise < 10% of the overall modal mineralogy, with early forming phases being the major phenocrysts. These commonly include olivine and plagioclase, however, in evolved MORB magmas clinopyroxene can be a prevalent phenocryst phase. Although less common, porphyritic lavas having much more abundant phenocrysts are also observed. Because MORB crystallize relatively quickly even the first formed crystals are commonly quite small (< a few mm) and thus called "microphenocrysts". Large (cm-sized) phenocrysts are rare and the presence of such large crystals is often due to the entrainment of xenocrysts (foreign crystals that formed in another magma and were incorporated into the lava prior to eruption. Textures that show intergrowth of multiple phases (both in the phenocryst assemblage and in the groundmass) are indicators of phases that crystallized cotectically (simultaneously). Density differences among these phases and circulation in a magma chamber may also cause glomeroporphyritic textures (groups of phenocrysts that are "stuck" together) .

As magma chemistry changes (evolves) through crystallization or magma recharge, early forming phenocrysts can become unstable in the changing liquid composition or temperature. This will result in the growth of new chemical zones around the edges of the existing crystal (crystal zoning) or in some cases phenocrysts may begin to be resorbed into the magma resulting in disequilibrium textures. Rounded anhedral to subhedral grains are commonly observed in olivine phenocrysts that become unstable in evolving magmas. Disequilibrium plagioclase can become sieve-textured displaying a "moth-eaten" appearance. Plagioclase and pyroxene typically display compositional zoning in response to changing magma chemistry, but such zoning is less-well preserved in olivine (solid-solution changes in chemistry occur more rapidly and completely in olivine compared to plagioclase or clinopyroxene).

Figure 5: Photomicrographs of example textures.

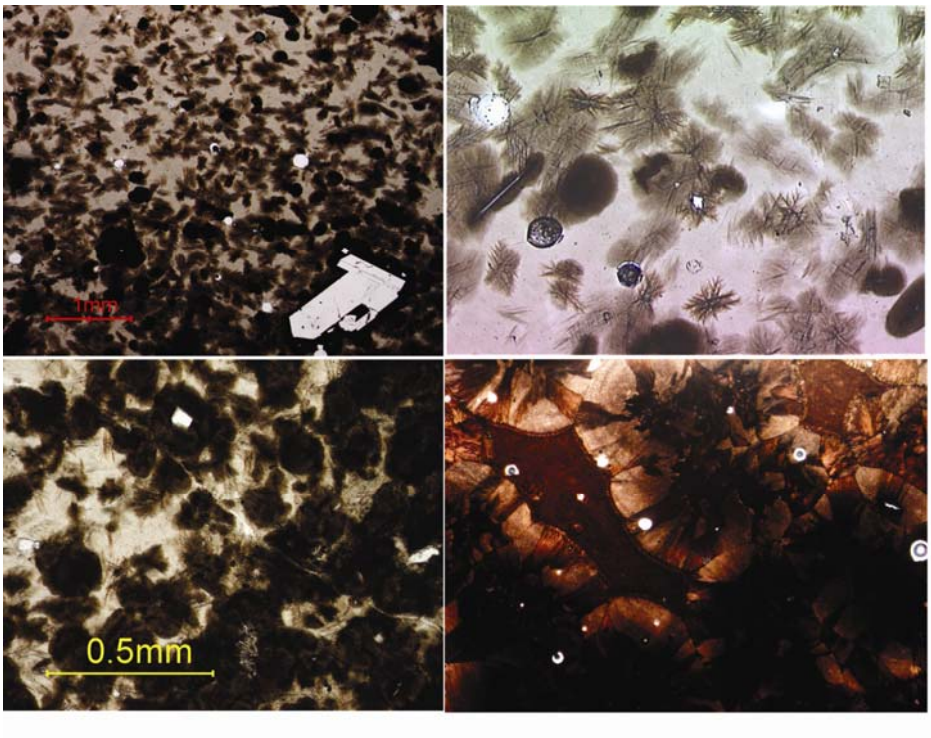

Figure 5a. (Top left) Quenched microlites in glass (Top Right) High magnification view of the top left photo. (Bottom Left) Quenched glass and microlites of plagioclase forming a variolitic texture. (Bottom Right) High magnification view of a variolitic texture.

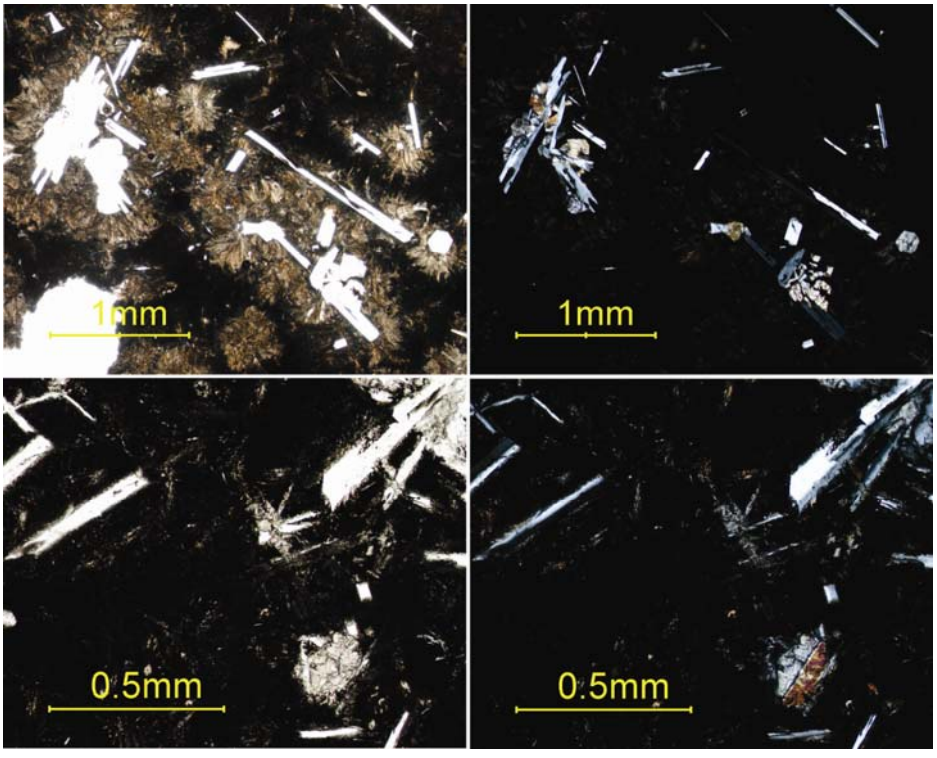

Figure 5b.
(Top) Fascicular to variolitic textures surrounding cotectically intergrowths of plagioclase feldspar and olivine. Shown in both plain-polarized light (right) and cross-polarized light (left).

(Bottom) FeTi basalt showing cotectic intergrowth of clinopyroxene and plagioclase feldspar. Shown in both plain-polarized light (right) and cross-polarized light (left). Pigeonite is visible in the lower right hand corner as a twinned grain.

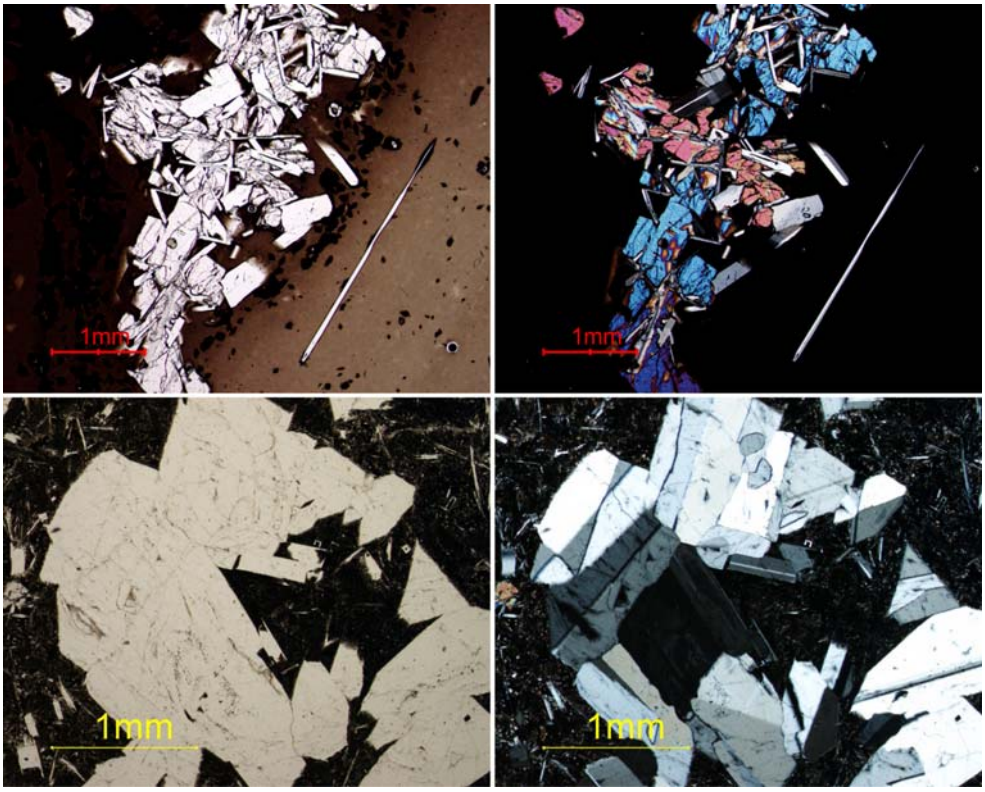

Figure 5c. (Top) Crystal clot showing cotectically intergrown olivine and plagioclase in both plane polarized light (left) and cross-polarized light. Olivine grains show embayments and grain shape indicative of resorption and disequilibrium.

(Bottom) Glomeroporphyritic crystal clot of plagioclase feldspar. Plain-polarized light shown at left and cross-polarized light shown at right.

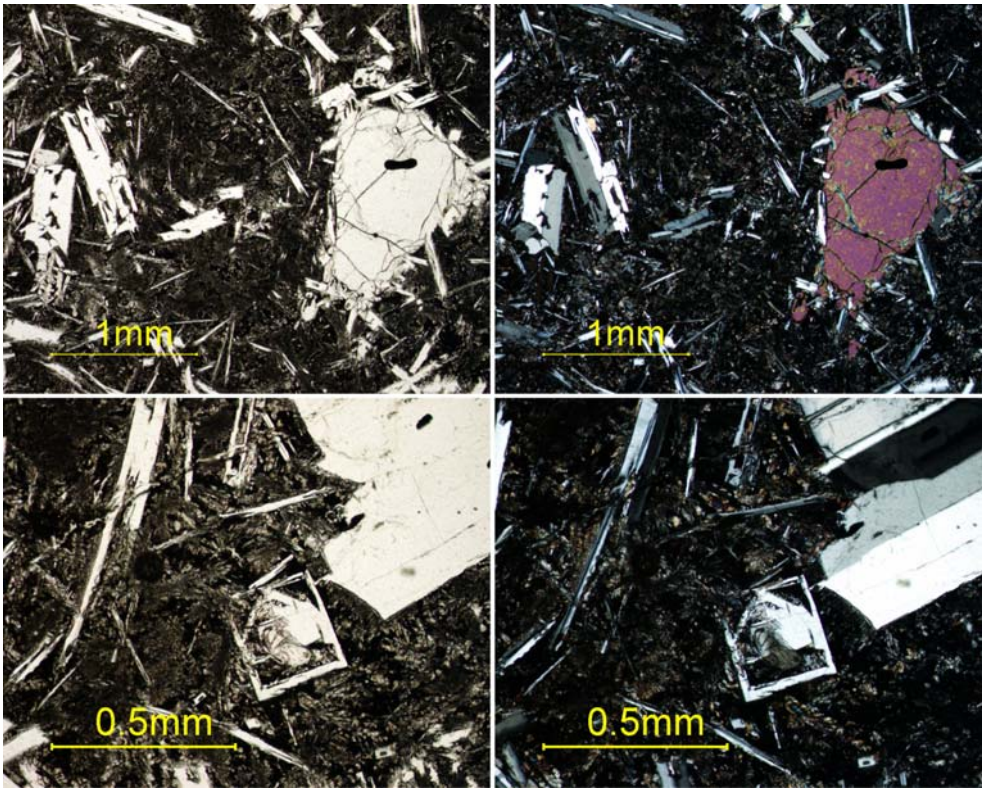

Figure 5d.
(Top) Olivine and plagioclase feldspar showing minor disesquilibrium textures. Plain-polarized light shown at left and cross-polarized light shown at right.

(Bottom) Swallowtail and skeletal plagioclase feldspar indicative of rapid undercooling and quench. Groundmass shows a fascilular to variolitic texture. Plain-polarized light shown at left and cross-polarized light shown at right.

Exercise: Thin-section Analysis of lavas from the southern Juan de Fuca Ridge

Samples
JdF90-DR12A-2
ALV-2268-1
T179-G7 or G8
JDF-90-DR13-3
T178-G4
T735-G12

Note that it can be very useful to first examine and describe the slide macroscopically by putting it on a sheet of white paper. It is generally a good idea to start your examination at the lowest magnification and proceed towards higher magnification. When examining the slide microscopically be sure to use both plain- and crossed-polars. Additionally, the provided chemistry can be used as a guide to probable mineral content.

1. ALV-2268-1
    a. What are the two major microphenocryst phases? Detail the observations you made to draw this conclusion.

    b. Several phenocrysts show a texture of cotectic (simultaneous) crystallization. Find an example of this and draw it.

    c. Examine the overall population of phenocrysts. Which of these phases do you think may have started crystallizing first? Explain the observation(s) that led you to this conclusion. (Tip: Consider differences in crystal morphology the associations in which crystals occur relative to one another when trying to determine the sequence of crystallization.)

    d. Examine the groundmass texture. You may want to increase the light intensity to get a good view. Describe (draw) and identify the most prevalent texture you observe.

2. JDF-90-Dr12a-2
    a. Examine the groundmass mineral phases and matrix (when examining the groundmass, you may want to intensify the transmitted light or engage the condenser lens and also utilize medium to high magnification). Describe and draw any textural features that are indicative of rapid quenching of this lava.

    b. This sample only has one phenocryst phase. What is it?

    c. Olivine occurs as a fine-grained groundmass phase. Is the sequence of crystallization in this sample consistent with the sequence you determined for sample ALV-2268-1? Why or why not?

3. T179-G7, 8 or 10: This MORB is composed primarily of three silicate mineral phases, opaque minerals and glass (both of the latter as part of the groundmass).

    a. Identify the three silicate phases that occur as phenocrysts or microphenocrysts. You may need to work a bit to distinguish the two mafic phases from one another. Be sure to note the observations you made to correctly identify the phases; an interference figure may be diagnostic in distinguishing the two mafic phases. (Tip: The best interference figures are seen in grains that don't change their appearance and color greatly with stage rotation in cross-polars. Look for a grain that is big enough and has low-order interference colors. Your high power objective should be fairly well centered to get a good interference figure on a small grain.)

    b. Describe the textural relationship(s) that exist between the phenocryst phases? What might you infer about the relative timing of crystallization of these phases?

    c. Describe and draw any textural features that are indicative of rapid quenching of this lava.

d. How does the crystallinity and relative abundance of phenocryts in this sample compare to that of JDF-90-DR12a-2? What might you infer about these two rocks from your observations? (Hint: think pre-eruption cooling history, not so much post eruption cooling history. You might also consider how the chemical compositions of these two samples differ, and a possible cause of that difference.)

4. T735-G12: This rock is also from the Juan de Fuca Ridge, but it is quite rare and unusual. Examine the major element chemistry in Table 1.

   a. Classify the rock type for this lava using Figure 6 and the given rock chemistry.

   b. Would you expect to find olivine in this rock? Explain?

   c. Describe the mineralogy of this lava. Using optical techniques, try to determine the composition of plagioclase present in this sample. Compare this plagioclase composition to the composition observed (or presumed) in one of the previously examined basalt samples. (Tip: The Michel-Levy Technique can be used to determine the composition of plagioclase feldspar. A description of this technique can be found in most Optical Mineralogy Textbooks.)

   d. Examine the vesicles. How do they compare in size and overall modal percent to the more primitive MORB samples? Are your observations consistent with the chemistry of this rock? Why or why not?

   e. Examine the groundmass. Note that overall it appears to be glassier compared to the more variolitic and fascicular textures seen in the basalts. Hypothesize a possible explanation for this observation?

f. This lava has a number of xenoliths and xenocrysts included in it. Find one (or more, preferably) and examine it. What is the mineralogy of the xenoliths? What do you think these xenoliths represent and where did they originate? Justify your answer.

g. Compare the textures observed in the xenoliths compared to the host rock. Describe each. Also closely examine the texture along the contacts between xenolith and host rock. Note any observations you make.

h. Hypothesize a possible origin for the xenoliths.

5. Complete full thin-section descriptions for JDF-90-13-3 and T178-G4. Be sure to note the following in your descriptions: phenocryst mineralogy, your best guess of the groundmass mineralogy, the approximate modal % of each phenocryst phase, and any textures indicating disequilibrium, condition/timing of crystallization or post eruptive cooling. Remember, it can be very useful to first examine and describe the slide macroscopically by putting it on a sheet of white paper. It is generally a good idea to start your examination at the lowest magnification and proceed towards higher magnification. When examining the slide microscopically be sure to use both plain- and crossed-polars.

6. The P-T phase diagram in Figure 7 shows the crystallization sequence for primitive basalt. In this kind of diagram, phase relationships of a single starting magma composition (in this case, that of primitive basalt) are investigated as variables of both pressure and temperature.

   a. Starting from the "all liquid" field of this diagram (a temperature greater than the liquidus temperature), draw a cooling/crystallization path on the diagram for a magma that crystallizes at low pressure (less than 1 GPa), and one at higher pressure. Describe the predicted sequence of crystallization for each cooling/crystallization path.

b. Describe how the crystallization history of a primitive basalt differs in these two different cooling pathways?

c. Using the mineral and textural observations from your thin-sections (and your interpreted sequence of crystallization), at what range of pressures do you think the thin-section samples crystallized? Justify your answer.

7. Figure 8 is the four-component (Anorthite-Forsterite-Clinopyroxene-Quartz) phase diagram projected from the plane of plagioclase saturation [after Walker, 1979]. Plagioclase is assumed to be saturated and crystallizing in all fields. (Note that this is a different kind of phase diagram than that of Figure 7. In this diagram composition and temperature are the variables and the pressure is held constant.) Point A and B represent starting compositions for liquid lines of decent (LLD) discussed below. Points P and E are invariant reaction (P) and eutectic (E) points, respectively.

   a. Draw onto Figure 8 the liquid line of decent that you would expect from magma that crystallizes, starting from either point A or point B. (Draw one LLD from each point.) Describe the sequence of crystallization for each LLD? (Remember, plagioclase is assumed to be crystallizing in all cases on this diagram.)

   b. Use the phase relations you observed in the thin-sections to approximate where each of the samples would plot on your proposed liquid line of decent, and plot them on Figure 8. Note that although you may not have found it, the mineral pigeonite (sub-calcic clinopyroxene) occurs in sample JdF-90-DR13-3.

   c. From this information, place the samples in order from most primitive to most evolved.

   d. Consider the chemistry and petrography of sample T178-G4; it is a ferroandesite. One possible petrogenetic origin for this sample could be a mix between a basaltic melt and a silicious melt. Draw a mixing line onto Figure 8 that connects samples T179-7 and T735-G12. Predict the mineralogy of a sample produced by a mix of these two compositions. How does your prediction compare to the observed mineralogy of sample T179-G4? Hypothesize at least two petrographic observations that might

be indicative of magma mixing and found in a sample formed by mixing of these two end-member magmas.

8. Using the program Excel and Table 1, plot the major oxide compositions of your samples against the MgO wt.%, and the total alkali content vs. the SiO_2 wt.%. Then answer the following questions.

a. On most regular Harker diagrams the major oxides are plotted against SiO_2 wt. %. Why is MgO plotted on the x-axis for MORB lava suites instead?

b. Using your Excel diagrams and the information from your petrographic analysis of the thin-sections, how does MgO change with increasing evolution (differentiation) of the magma?

c. Describe the manner in which each of the other major oxide concentrations change with increasing chemical evolution of the melt. Hypothesize why these particular trends exist in the data ?

Table 1

Sample	DR12A-2	T179-G7	2268-1	DR13-3	T178-G4	735-12
[1]Type	DR	TIB	ALV	DR	TIB	TIB
Latitude	45 10.5	44 34.88	44 39.48	44 26.3	44 34.88	44 30.00
Longitude	-130 9.6	-130 21.60	-130 21.37	-130 28.2	-130 24.28	-130 28.42
SiO2 (wt.%)	50.1	50.8	50.3	49.9	53.7	66.9
TiO2	1.21	2.13	1.58	2.98	1.89	0.786
Al2O3	15.7	13.7	14.6	12.6	14.0	12.1
[2]FeO*	9.39	12.8	10.8	15.4	11.6	7.64
MnO	0.21	0.25	0.20	0.27	0.22	0.15
MgO	8.23	6.43	7.47	5.17	4.89	0.585
CaO	12.5	10.7	12.4	9.74	8.82	3.41
Na2O	2.33	2.88	2.43	2.98	3.29	4.55
K2O	0.08	0.16	0.10	0.22	0.49	1.16
Total	99.7	100.1	99.9	99.2	99.3	98.6

notes:
1. Dr=sampled by dredge, ALV=sampled using the submersible ALVIN, TIB=sampled using the ROV Tiburon

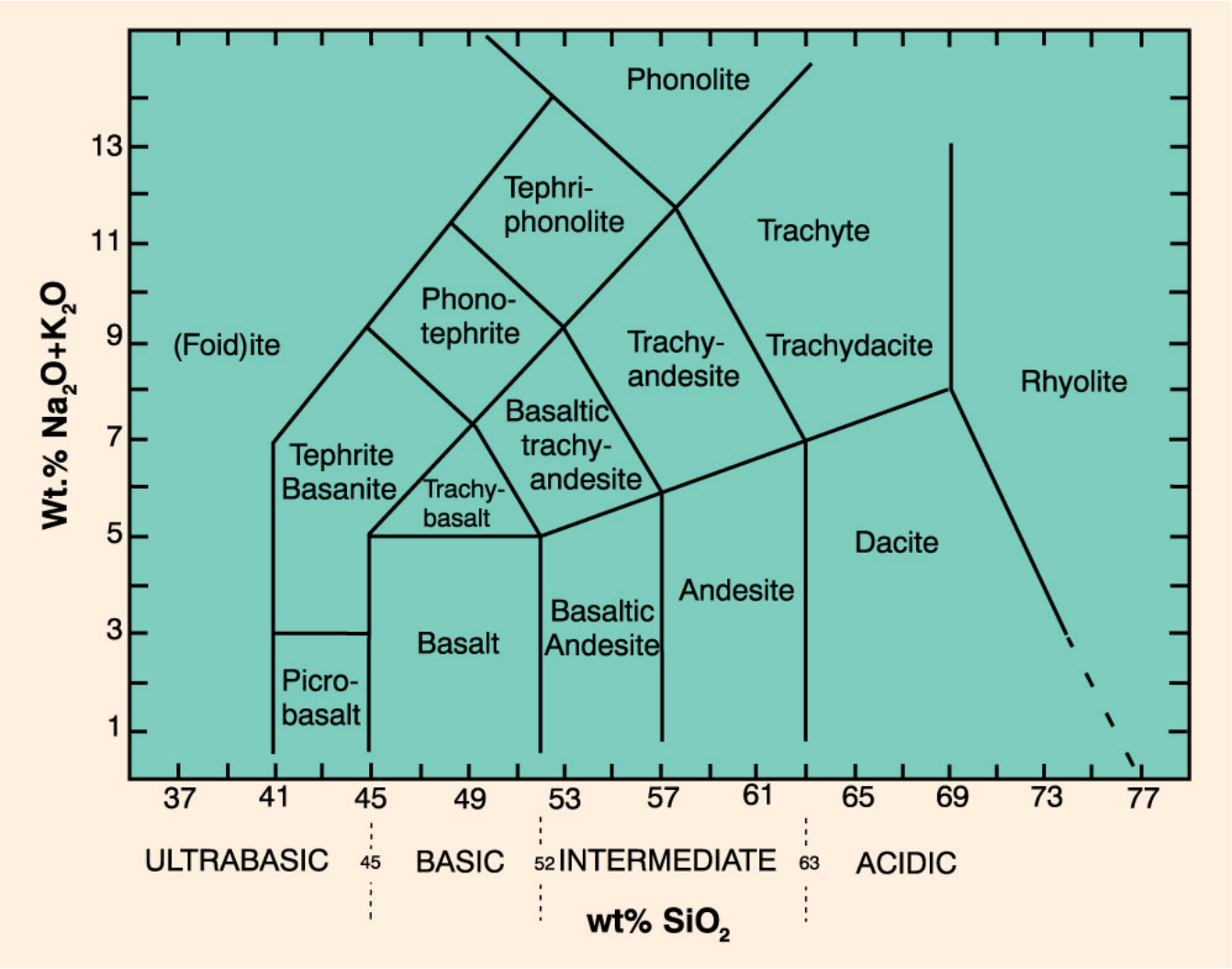

Figure 6. Total alkali vs silica classification diagram (IUGS Classification)

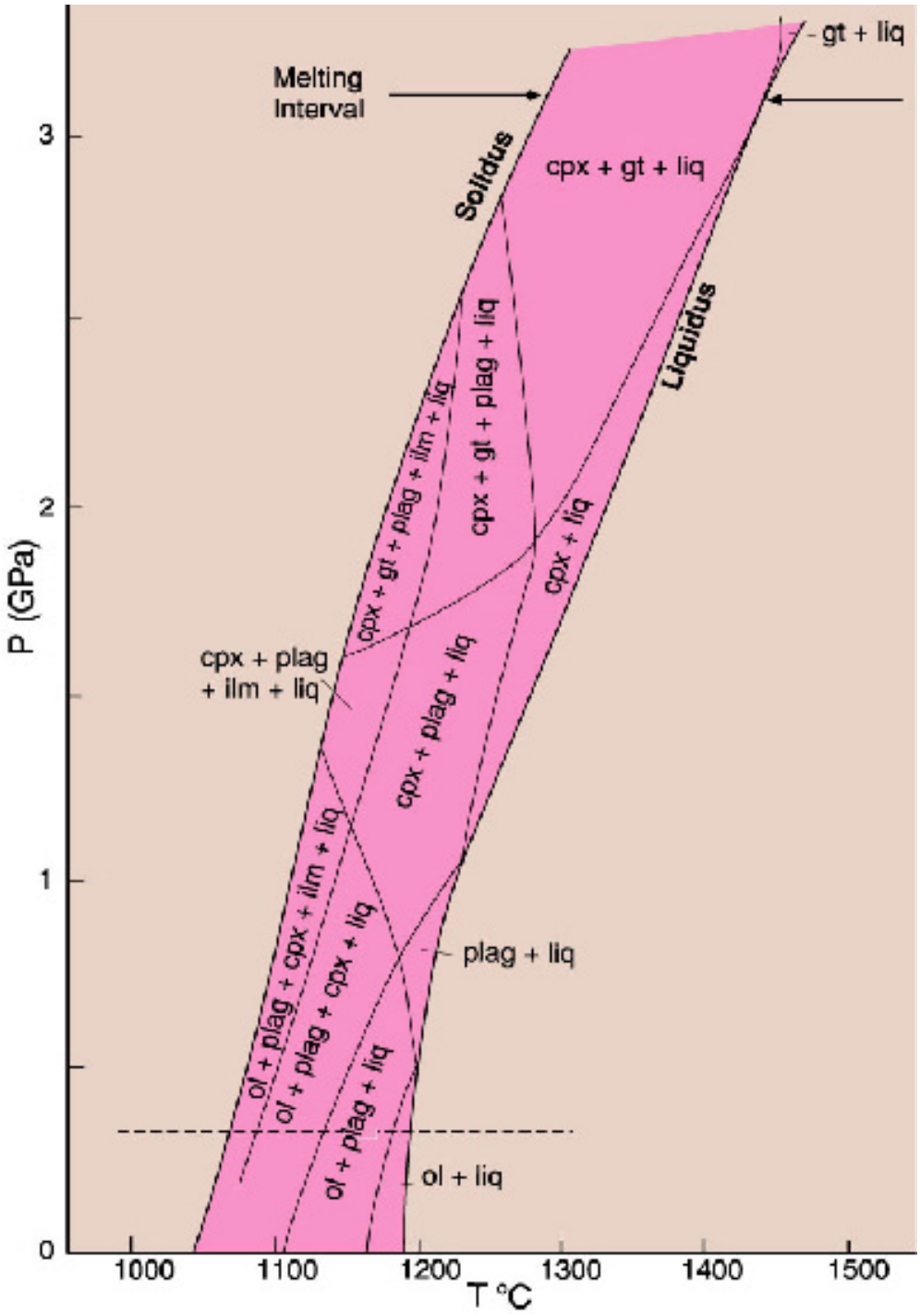

Figure 7. Pressure-Temperature phase diagram for crystallization of a Primitive MORB (composition is a constant in this diagram). [after Thompson, 1973]

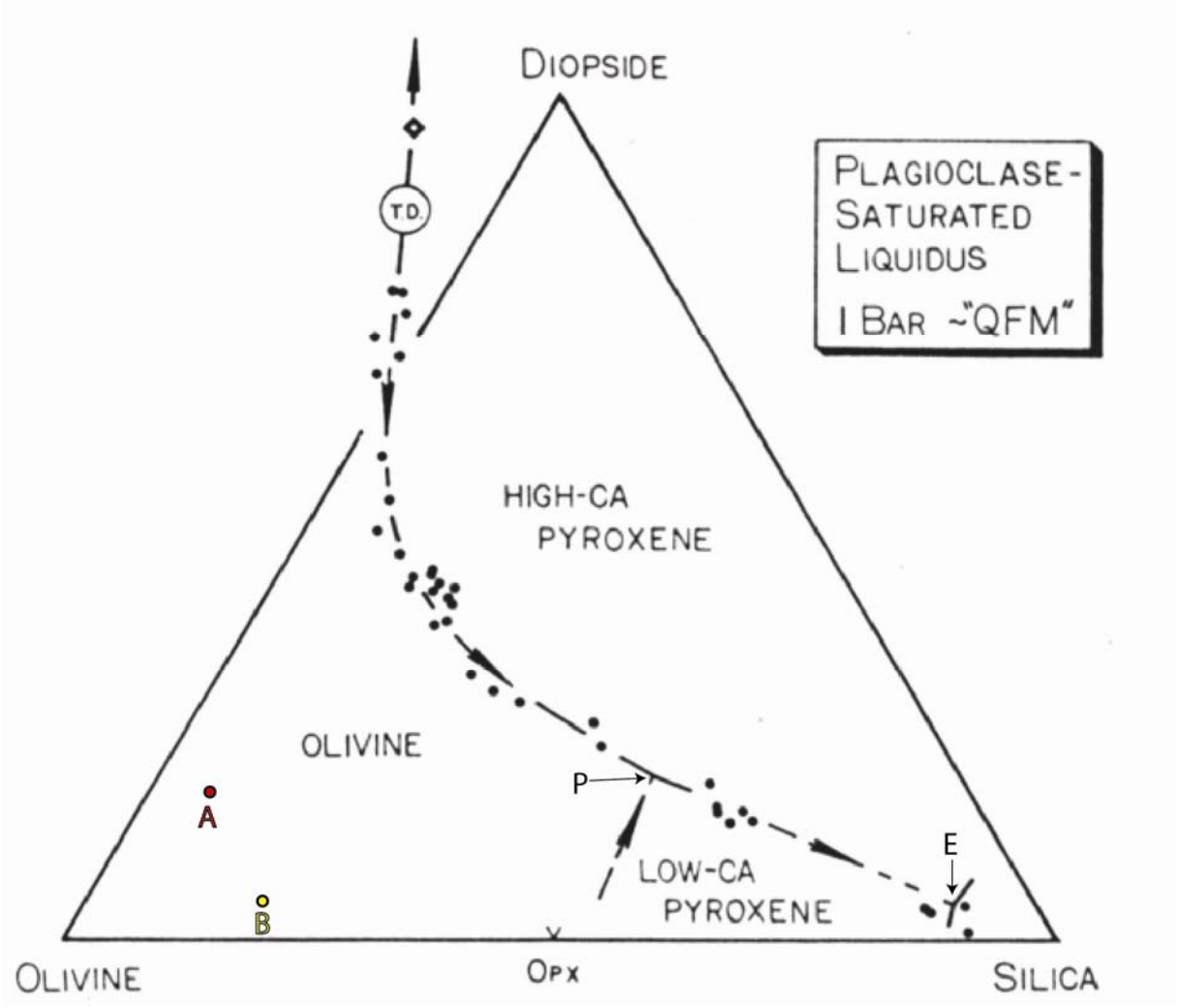

Figure 8. Diagram of the olivine-plagioclase-quartz-augite quarternary system, projected from the plane of plagioclase saturation onto the plane Olivine-quartz-augite [Walker et al., 1979]. System is plotted in mole components. Points A and B are starting compositions referred to in the text. Point P is a peritectic point in this system while Point E is a eutectic point. Note that since this publication of this diagram refined (and slightly more complex) phase-relations have been determined for this system and published (see Grove and Bryan, 1983, for example). This older version was chosen for ease of interpretation, however, more recently determined phase relations are used in modern research.

References

Bryan, W.B. (1883), Systematics of modal phenocryst assemblages in submarine basalts: Petrologic implications, *Contributions to Mineralogy and Petrology*, *83*, 62-74.

Embley, R.W., W.W. Chadwick, M.R. Perfit, and E.T. Baker (1991), Geology of the northern Cleft segment, Juan de Fuca Ridge: Recent lava flows, seafloor spreading, and the formation of megaplumes, *Geology*, *19*, 771-775.

Embley, R.W. and D.S. Wilson (1992), Morphology of the Blanco Transform fault zone-NE Pacific: implications for its tectonic evolution, *Marine Geophys. Res*., *14*, 25-45.

Embley, R.W. and W.W. Chadwick (1994), Volcanic and hydrothermal processes associated with a recent phase of seafloor spreading at the northern Cleft segment: Juan de Fuca Ridge, *J. Geophys. Res*., *99*, 4741-4760.

Fornari, D.J., R.M. Haymon, M.R. Perfit, T.K.P. Gregg, and M.H. Edwards (1998), Geological characteristics and evolution of the axial zone on fast-spreading mid-ocean ridges: formation of an axial summit trough along the EPR, 9°-10° N, *J. Geophys. Res*., *103*, 9827-9855.

Grove, T.L. (1990), Cooling histories of lavas from Seroki Volcano, in *Proc. ODP, Sci. Results, V. 106/109*, edited by Detrick, R., Honnorez, J., Bryan, W.B., and Juteau, T., College Station, TX, 3-8

Grove, T. L., and Bryan, W. B. (1983). Fractionation of pyroxene-phyric MORB at low pressure; an experimental study. *Contributions to Mineralogy and Petrology*, *84*(4), 293-309. Retrieved March 13, 2007, from GeoRef database.

Head, J.W., L. Wilson, and D.K. Smith (1996), Mid-ocean ridge eruptive vents: evidence for dike widths, eruption rates, and evolution of eruptions from morphology and structure, *J. Geophys. Res*., *101*, 28265-28280.

Kappel, E.S. and W. B. Ryan (1986), Volcanic episodicity and a non-steady-state rift valley along northeast Pacific spreading centers: evidence from SeaMARC I, *Jour. Geophys. Res*., *91*, 13925-13940.

Morse, S.A. (1980) *Basalts and Phase Diagrams*, Springer-Verlag, New York.

Natland, J.H. (1980), Crystal morphologies in basalts dredged and drilled from the East Pacific Rise near 9°N and the Siqueiros Fracture Zone. In *Init. Repts. DSDP, vol. 54* edited by Rosendahl, B.R., Hékinian, R., et al., Washington (U.S. Govt. Printing Office), 605-634.

Normark, W.R., J.L. Morton, R.A. Koski, D.A. Clague, and J.R. Delaney (1983), Active hydrothermal vents and sulfide deposits on the southern Juan de Fuca Ridge, *Geology, 11*, 158-163.

Normark, W.R., J.L. Morton, J.L. Bischoff, R. Brett, R.T. Holcomb, E.S. Kappel, R.A. Koski, S.L. Ross, W.C. Shanks III, J.F. Slack, K.L. Von Damm, and R.A. Zierenburg (1986), Submarine fissure eruptions and hydrothermal vents on the southern Juan de Fuca Ridge: Preliminary observations from the submersible Alvin, *Geology*, *14*, 823-827.

Normark, W. R., J. L. Morton, and S. L. Ross (1987), Submersible observations along the southern Juan de Fuca Ridge: 1984 *Alvin* program, *J. Geophys. Res.*, *92*, 11283-11290.

Perfit, M.R. and W. W. Chadwick, (1998), Magmatism at mid-ocean ridges: constraints from volcanological and geochemical investigations, in *Faulting and Magmatism at Mid-Ocean Ridges*, *Geophys. Monogr. Ser.*, vol. 106, edited by W.R. Buck, P. T. Delaney, J.A. Karson, and Y. LaGabrielle, pp. 59-116, AGU, Washington, D.C.

Perfit, M.R. and D.J. Fornari, (1983), Geochemical studies of abyssal lavas recovered by DSRV ALVIN from the eastern Galapagos Rift - Inca Transform - Ecuador Rift: II. Phase chemistry and crystallization history, *J. Geophys. Res.*, 88, 10,530-10,550.

PetDB-The petrological database of the ocean floor (n.d.), Data retrieved in January, 2006 from http://www.petdb.org.

Smith, M.C., (1999), Geochemistry of eastern Pacific MORB: Implications for MORB petrogenesis and the nature of crustal accretion with the neovolcanic zone of two recently active ridge segments, Ph.D dissertation, 189 pp., Univ. of Fl., Gainesville, Fl..

Smith, M. C., M.R. Perfit, and I. R. Jonasson (1994), Petrology and geochemistry of basalts from the southern Juan de Fuca Ridge: controls on the spatial and temporal evolution of mid-ocean ridge basalt, *J. Geophys. Res.*, *99*, 4787-4812.

Stakes D. S., M. R. Perfit, M. A. Tivey, D. W. Caress, T. Ramirez, and N. Maher (2006), The Cleft revealed: Geologic, magnetic, and morphologic evidence for construction of upper oceanic crust along the southern Juan de Fuca Ridge, *Geochem. Geophys. Geosyst.*, *7*, Q04003, doi:10.1029/2005GC001038.

Thompson, R. N. (1973). One-atmosphere melting behaviour and nomenclature of terrestrial lavas. *Contributions to Mineralogy and Petrology, 41*(3), 197-204. Retrieved March 13, 2007, from GeoRef database.

Walker, D., T. Shibata, and S.E. DeLong (1979). Abyssal tholeiites from the oceanographer fracture zone; II, phase equilibria and mixing. *Contributions to Mineralogy and Petrology*, *70*(2), 111-125. Retrieved March 13, 2007, from GeoRef database.

Wilson, D. S. (1988), Tectonic history of the Juan de Fuca Ridge over the last 40 million years, *J. Geophys. Res.*, *93*, 11863-11876.

Wilson, D.S., R.N. Hey, and C. Nishimura (1984), Propagation as a mechanism of reorientation of the Juan de Fuca ridge, *J. Geophys. Res.*, *89*, 9215-9225.